INSTRUMENT SCIENCE REPORT

FOC-087

TITLE: The New *f*/96 Geometric Correction Models

AUTHOR: P. Greenfield **DATE:** 12 September 1995

ABSTRACT

Described are the new geometric distortion models determined for the post-COSTAR *f*/96 relay based on multiple, overlapping observations of crowded star fields. New distortion models were determined for the following *f*/96 formats: 512*z*×1024, 512×512, 256×1024, 256×256, and 128×128 using the method outlined in the previous Instrument Science Report FOC-086. Unlike the previous observations, the offsets between exposure appear to be as expected. The quality of the fits are good despite an apparent change of ~0.16% in plate scale over the course of all the observations. The consistency of fit star positions with the previous model is good. The consistency of the distortion fit with the previous 512×512 distortion fit using the new method is very good whereas the consistency with the previous 512*z*×1024 fit is less so. The evidence is strong that the photometric variations at the scan line beginning are not a direct result of distortion.

DISTRIBUTION:

FOC Project:	B.G. Taylor, R. Thomas
IDT:	R. Albrecht, C. Barbieri, A. Boksenberg, P. Crane, J.M. Deharveng, M.J. Disney, P. Jakobsen, T. Kamperman, I.R. King, C. Mackay, G. Weigelt.
SSD:	C. Cox, W. Hack, R. Jedrzejewski, A. Nota, All Instrument Scientists
SSG:	P. Greenfield, P. Hodge. R. White
SESD:	M. Miebach, W. Safley
Dir. Office:	F. Macchetto
ST/ECF:	P. Benvenuti, R.A.E. Fosbury, R.N. Hook, A. Caulet

1. Introduction

This report documents the derivation of the new geometric correction calibration files being used for FOC calibration pipeline processing. The method used is basically that reported in Instrument Science Report FOC-086 with some minor changes. Only a very brief outline of the method will be given here with elaboration given only for those aspects different from the original report. Readers are expected to refer to that report for details on the theory and rationale for the approach used. An accompanying Instrument Science Report will document the software written to derive the models.

The basic method consists of spatially overlapping observations of a crowded star field. Presuming the image offsets are known to high accuracy and assuming the relative star positions are constant for the series of observations, it is in principle possible to determine the underlying distortion model as long as the spatial density of stars is sufficiently high to sample the variations in distortion well enough. No a priori knowledge is needed for the relative star positions; they are determined from the fit along with the distortion model parameters. Reseau positions are only used to register the new distortion model with the old model, otherwise they are irrelevant The previous two-dimensional polynomial representation for the distortion model has been replaced by a two-dimensional spline representation to better fit the high spatial frequency components of the distortion.

The star field selected was the center of 47 Tucanae, which experience has shown can provide a sufficiently dense field of relatively uniform brightness stars. This last characteristic is particularly important since just a few very bright stars can render significant parts of the field of view useless because of saturation effects in the FOC.

2. The Observations

The data were obtained from proposal 5750 executed on 11 November 1994. Two previous attempts to run this program (as proposal 5521) failed; the first because of a faulty guide star, the second because the necessary warm up time for optimum stability had not been inserted (a minimum of 4 hours after high voltage switch-on). Table 1 lists the exposure information for the proposal. The offset column represents the relative offset in RA and DEC in arcseconds of that exposure to the default position.

In principle the overlapping exposures only need to be done for the full format and the star positions derived used to determine the distortions for all the other formats by means of only one exposure per format. There are two reasons this was not done for all the formats. The first is that determining the star positions for the full format results in somewhat poorer positions because of the use of the zoomed pixel mode. We decided to fit the star positions independently for the 512×512 format to get a higher quality fit. A second important reason to use overlapping exposures, even when not necessary to determine the position of the stars, is to increase the effective density of samples of the distortion. Ideally, we would prefer an even higher density of stars than

Exposure	Format	Offset in RA (")	Offset in DEC (")	Filter	Exp. Time (s)	Target
x2jh0101t	512z×1024	N/A	N/A	N/A	3000	DARK
x2jh0102t	512×512	N/A	N/A	N/A	969	LED
x2jh0103t	512z×512	0	0	F220W	597	47 Tuc
x2jh0104t	512z×1024	3.471	–3.529	F220W	597	47 Tuc
x2jh0105t	512z×1024	–3.529	–3.471	F220W	597	47 Tuc
x2jh0106t	512z×1024	–3.471	3.529	F220W	597	47 Tuc
x2jh0107t	512z×1024	3.529	3.471	F220W	597	47 Tuc
x2jh0108t	512z×1024	0	0	F220W	597	47 Tuc
x2jh0109t	512×512	1.735	–1.764	F220W	418	47 Tuc
x2jh010at	512×512	–1.765	–1.735	F220W	597	47 Tuc
x2jh010bt	512×512	–1.735	1.765	F220W	597	47 Tuc
x2jh010ct	512×512	1.765	1.735	F220W	597	47 Tuc
x2jh010dt	512×512	0,0	0	F220W	597	47 Tuc
x2jh010et	256×256	1.000	–0.008	F220W	597	47 Tuc
x2jh010ft	256×256	–1.000	0.008	F220W	597	47 Tuc
x2jh010gt	256×256	0	0	F220W	597	47 Tuc
x2jh010ht	128×128	0	0	F220W	654	47 Tuc
x2jh010it	128×128	–1.000	0.008	F220W	717	47 Tuc
x2jh010jt	256×1024	0	0	F220W	597	47 Tuc
x2jh010kt	256×1024	–1.000	0.008	F220W	597	47 Tuc
x2jh010mt	512z×1024	0	0	F220W	600	47 Tuc
x2jh0101t	512z×1024	N/A	N/A	N/A	900	LED

Table 1. A summary of the exposures for proposal 5750.

is observed for 47 Tuc (we know of no target which has a higher density of stars this bright). By using overlapping exposures we effectively increase the density a factor equal to the number of different offsets. This was done for the smaller formats for this reason (the 128×128 format would only have had about 20 usable stars in the fields without use of more offsets for example).

These offsets were chosen (by use of POSTARG) to give approximately 250 pixel offsets in x and y in the image for the full format (and half that for the 512×512 format) so that the four offset images were placed half way towards each of the four corners of the centered exposure. As it was, the roll angle was such that the y-axis was virtually aligned with north (position angle of $0.^{\circ}715$).

3. Data Analysis and Results

The analysis was carried out as described in FOC-086 with the following exceptions. First, there were two bugs found in the star matching program one of which effectively excluded from the stars used those used in manually matching pairs of stars between different images. Other than reducing the number of stars used in the fit, it had no systematic effect on the previous results (the fraction of lost stars was typically ~10% for the largest formats but was generally larger for smaller formats). The second bug resulted in a few stars being present twice in the star lists. Both bugs were fixed and the results presented here were not affected by them. Second, the results derived in the first report did not use any weighting for the parameter fits. Weighted versions of the fitting programs were developed and those versions were used for all video formats that did not use the zoomed pixel mode. The weighting was based on the total counts of each star and the weighting function used is that derived from Figure 2 in ISR FOC-086. Third, all indications are that the actual image offsets were very near those that were commanded. Thus it was not necessary to try to determine the offsets based on reseau positions as was done for the previous report. In other words, the analysis was carried out as planned this time without using any workarounds. Fourth, a new program was written to exclude stars from full format exposures suspected of being overflowed, and to exclude all stars closer than 4 pixels to another star in the list of stars.

As in the previous report, the adopted plate scale is 0.01435 arcsec per normal pixel for all the distortion models (the plate scale is purely arbitrary, the value chosen is close the average plate scale in the uncorrected images and is the value adopted for the previous post-COSTAR geometric correction models). The orientation of the corrected image is set by making match the predicted orientation given in the exposure headers (again, this is arbitrary; it was chosen to remain consistent with past models). The relative position of the geometrically corrected full format was chosen so that the reseau locations matched up on average with those of the previous distortion corrections. The relative position of all the other formats was forced to result in alignment with the full format after accounting for the assumed relative offset between the formats (e.g., 256, 256 pixels for the 512×512 format relative to the full format). These conventions ensure the consistency of alignment and plate scale between all formats, something that has not been precisely true for previous geometric correction models where different formats ended up with slightly different orientations and offsets. But note that this enforced consistency does not eliminate misalignments or scale changes between images (of the same or different formats) due to changes in the intrinsic distortion over time).

The spline knot locations are identical to those used in FOC-086 for all the formats except 128×128 which was not done in the previous report. Because of the small number of points in that format, a two-dimensional polynomial model was used instead for the distortion. (This is a considerable improvement over the previous case for there was no model whatsoever given the inadequate number of reseaux present to determine a model.) Table 2 lists the knot locations used for

each format. Table 3 lists the number of data points and number of stars involved in the fit for each format.

Format	x knot Positions	y knot Positions
512*z*×1024	127	302
	240	703
	260	
	331	
	402	
	439	
	473	
512×512	159	142
	341	370
	420	
	467	
256×256	108	324
	213	710
256×1024	128	128

Table 2. A list of the x and y knot positions for all the formats that use spline fits.

Format	Data Points	Stars
512*z*×1024	4703	1623
512×512	1544	546
256×256	242	N/A
128×128	39	N/A
256×1024	577	N/A

Table 3. The number of data points and stars used in the model fits for each format. The last three formats do not fit star positions, only the distortion parameters.

3.1. 512 zoomed×1024

The distortion model for the full format was obtained using an unweighted fit. The rms residuals for x (in normal pixel units) and y were 0.33 and 0.28 pixels. The plot of the residual vectors is shown in Figure 1. No spatial correlation of residuals is evident suggesting that the high fre-

quency components have been adequately fit. The resulting model was then applied to correct the positions obtained from reseaux fits for the full format LED image (x2jh010mt) to undistorted coordinates. A linear transformation to match the undistorted reseau positions with the reference positions used previously to determine distortion models was determined by a least squares fit, and then applied to the reseaux positions to produce a vector plot of residuals. This plot is shown in Figure 2. There are no clear large scale systematic effects in the residuals. The rms residuals in *x* and *y* are 1.03 and 0.79 pixels. Although smaller than obtained for the previous report, they are still at least a factor of 2 or 3 larger than expected. I have no explanation for a discrepancy of this size. The linear transformation that was fit was consistent with a simple rotation and translation with no evidence for a scale error or skew (the linear transformation fit resulted in a scale change of 0.2% and a rotation of 0.°09). This strongly suggests that the offsets between the exposures was very close to that commanded.

One clear test of the reliability of the modeling process can be done by comparing the fit positions for the stars for the current data with those obtained for the fit reported in FOC-086. Since the relative orientation between the two observations is known, and the same star can be used to determine the relative offset, the transformation between the two coordinate systems can be determined a priori. This was done and then a program to match stars between the two lists was run. After matching the stars, a linear orthogonal transformation was fit to minimize the residual differences in position. Ideally, the fit transformation would show no offset, rotation, or scale change. But detector plate scale changes between different high-voltage switch-ons are not unusual and in fact the resulting fit shows a effective change of 0.7% between the two sets of positions. The effective rotation is less than 0.°5. The residual rms in *x* and *y* were 0.48 and 0.55 pixels which should be considered reasonably good agreement considering the presence of random errors in both sets of data (this level of residuals implies intrinsic position errors on the order of 0.3-0.4 pixels for the full format fits). If a linear transformation between the two coordinate systems that allows skew is fit, then the *x* and *y* rms residuals become 0.37 and 0.49 pixels indicating there was a small amount of skew present in the old solution left after matching to the reseau grid.

3.2. 512×512

The fit for the 512×512 format produced significantly smaller residuals. The rms residuals for *x* and *y* were 0.19 and 0.23 pixels. The residual vectors are shown in Figure 3. The star positions determined here were compared to those determined from the full format fit in a similar way to those done for the old and new observations. Using only the a priori transformation between the coordinates (only an offsets since the orientation is presumably identical) the *x* and *y* rms residuals are 0.34 and 0.35 pixels. Allowing a linear orthogonal transformation reduced these residuals only slightly to 0.32 and 0.26 respectively. These independent determinations of the star positions agree quite remarkably and are consistent with the values seen for the fit residuals, i.e., the residu-

als of ~0.3 for the 512*z*×1024 fit and ~0.2 for the 512×512 fit. That means it is possible to do relative astrometry on crowded fields to the 3 mas level using this technique.

3.3. 256×256

The fit for the 256×256 format used the positions for the stars obtained from the 512×512 fit to determine the spline coefficients for this format. The resulting rms residuals for *x* and *y* were 0.35 and 0.44 pixels. The plot of the residual vectors is shown in Figure 4. The residuals are higher here presumably in part because of the contribution of the errors in the previously fit star positions.

3.4. 128×128

The fit for the 128×128 format used a simple two-dimensional polynomial model for the distortion. The rms residuals for *x* and *y* were 0.59 and 0.39 pixels. The plot of the vector residuals is shown in Figure 5.

3.5. 256×1024

The fit for this format used the star position solutions from the full format and resulted in *x* and *y* rms residuals of 0.35 and 0.38 pixels. The residuals are shown in Figure 6.

4. Consistency of the Distortion Model

Figure 7 shows magnified vectors showing the differences between the 512×512 distortion model derived for ISR FOC-086 and the latest distortion model. As can be seen, the differences are not large and appear primarily as a small rotation. The consistency for this format should be considered very good. The consistency of the full format solutions is not as good and cannot be explained as a simple rotation (see Figure 8). This discrepancy may arise from the problem with determining the offsets of the images for the first set of data, but that seems unlikely since errors in the offsets should only apply a skew to the distortion, it should not introduce smaller scale changes. It is quite possible that the intrinsic distortion is changing from one high-voltage switch-on to another. The only way to be sure is to carry out another run of the distortion and plate scale proposal and determine if the fine scale features in the distortion are changing. The repeatability of the fit star positions strongly imply that the distortion model derived is valid for this high-voltage switch-on at the very least. For the moment, it must be considered an open issue.

5. Consistency of the Plate Scale

Since the proposal contains two observations taken in the same configuration and pointing taken several hours apart (x2jh0108t and x2jh010lt), it is possible to check the stability of the distortion by comparison of the star positions between the two images. The magnified difference vectors are shown plotted in Figure 9. Fitting a linear orthogonal transformation gives an effective plate scale change of 0.16% and rotation of $0\overset{\circ}{.}014$. The rotation is negligible, but the plate scale change is more significant and demonstrates that a long warm up time does not make the FOC perfectly sta-

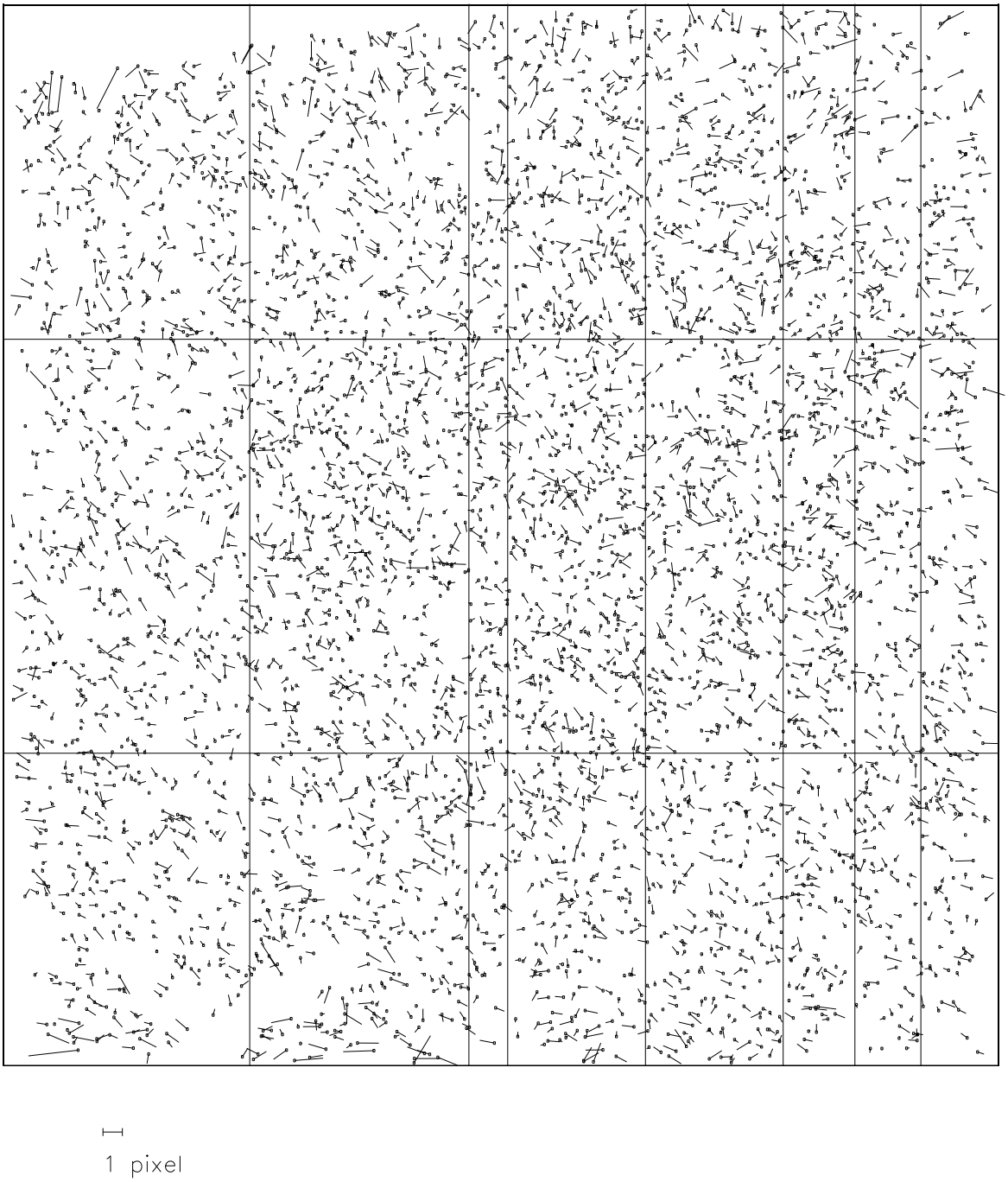

Figure 1. The residuals for the full format model. The residuals are shown as magnified vectors showing the difference between the measured star position and the model-predicted star position. The boxes designate the tails of the vectors. The vectors are placed at the position in the raw image corresponding to the measured star position. The overplotted horizontal and vertical lines show the location of the *x* and *y* knots that segment the spline fitting region.

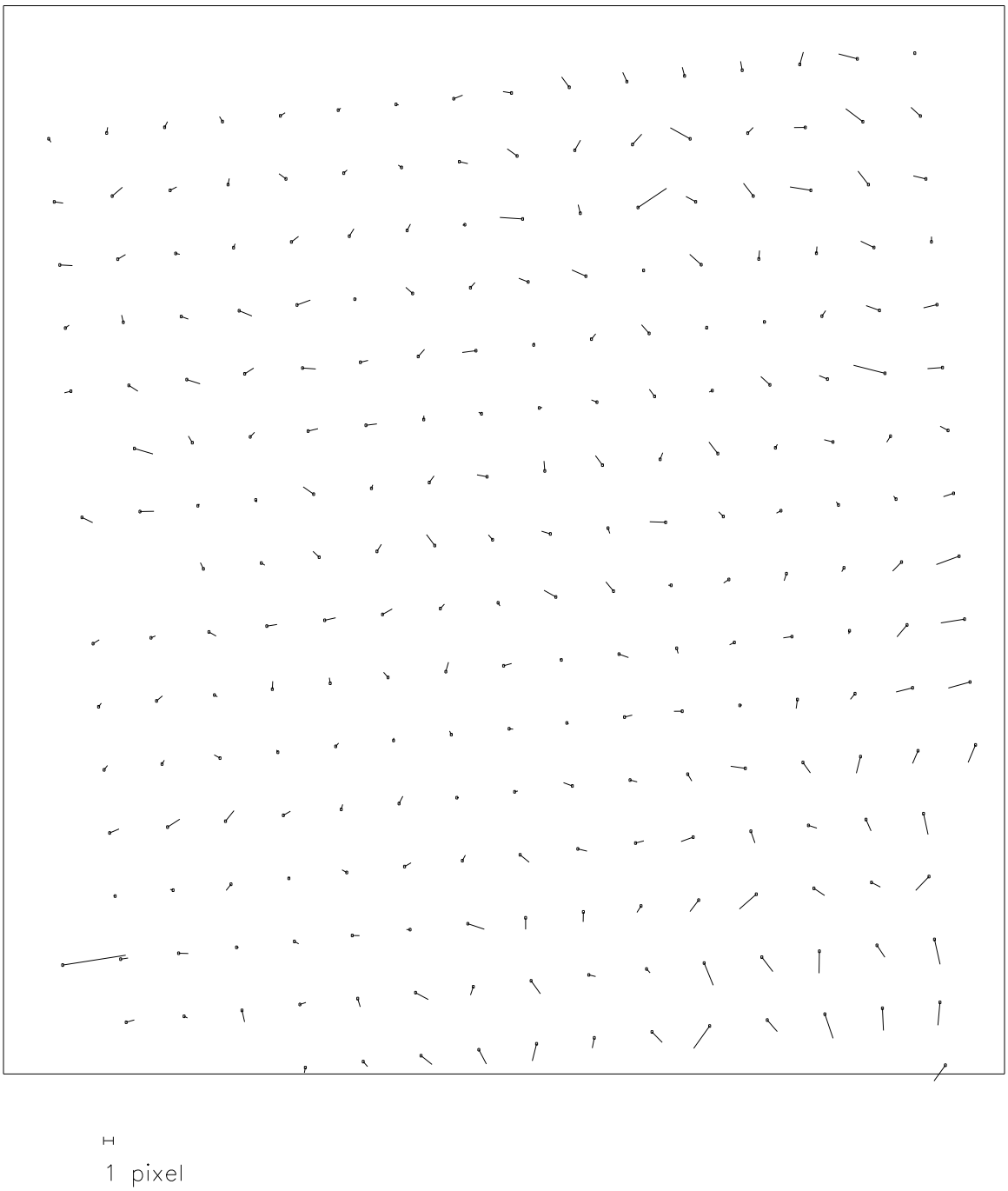

Figure 2. The difference between the predicted reseau positions and those determined by applying the geometric correction to the measured reseau positions. A linear transformation (including rotation, scale, and an offset) has been applied to the measured positions after geometric correction to best match the predicted positions.

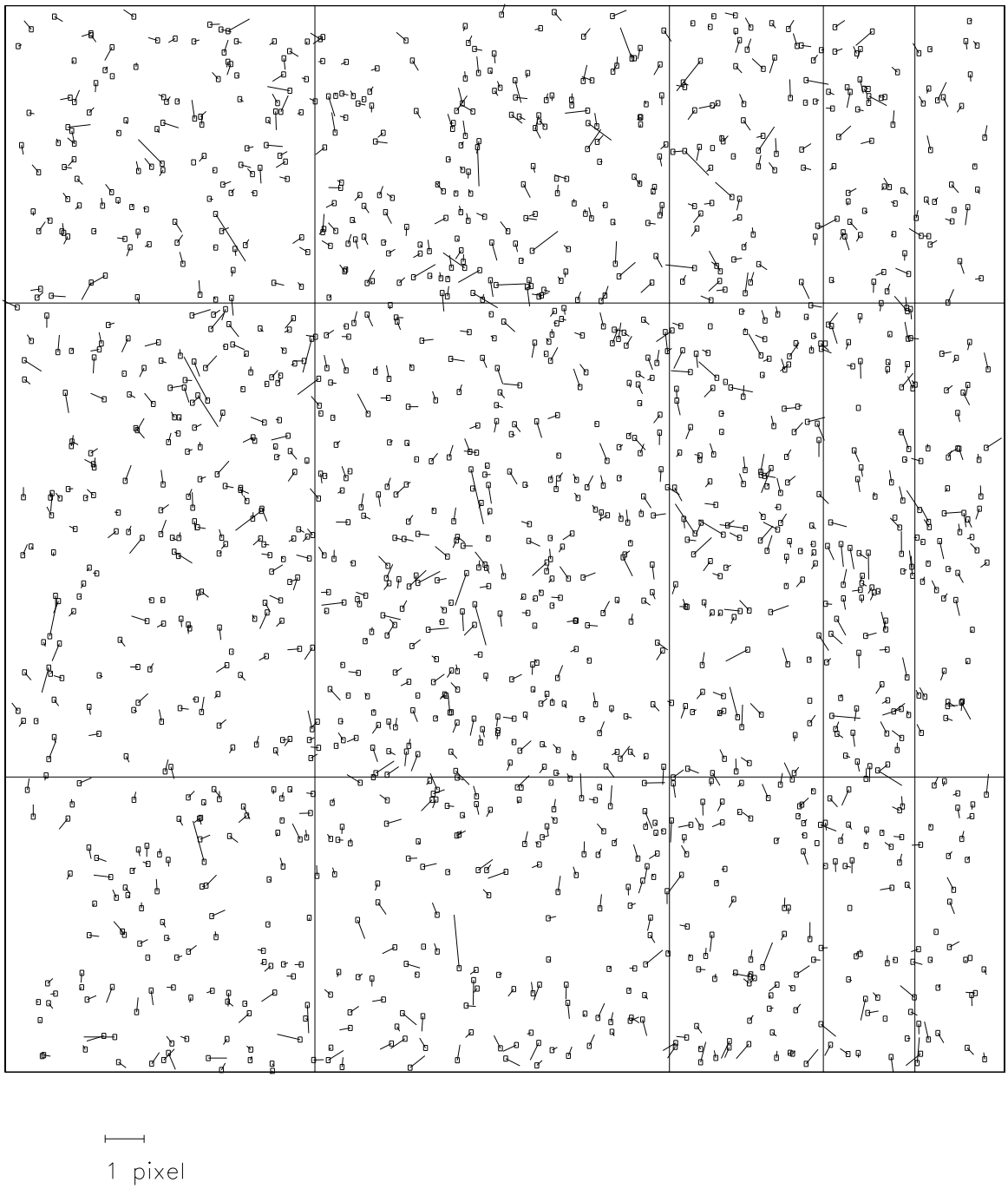

Figure 3. The residuals for the 512×512 model. The residuals are shown as magnified vectors showing the difference between the measured star position and the model-predicted star position. The boxes designate the tails of the vectors. The vectors are placed at the position in the raw image corresponding to the measured star position. The overplotted horizontal and vertical show the location of the *x* and *y* knots that segment the spline fitting region.

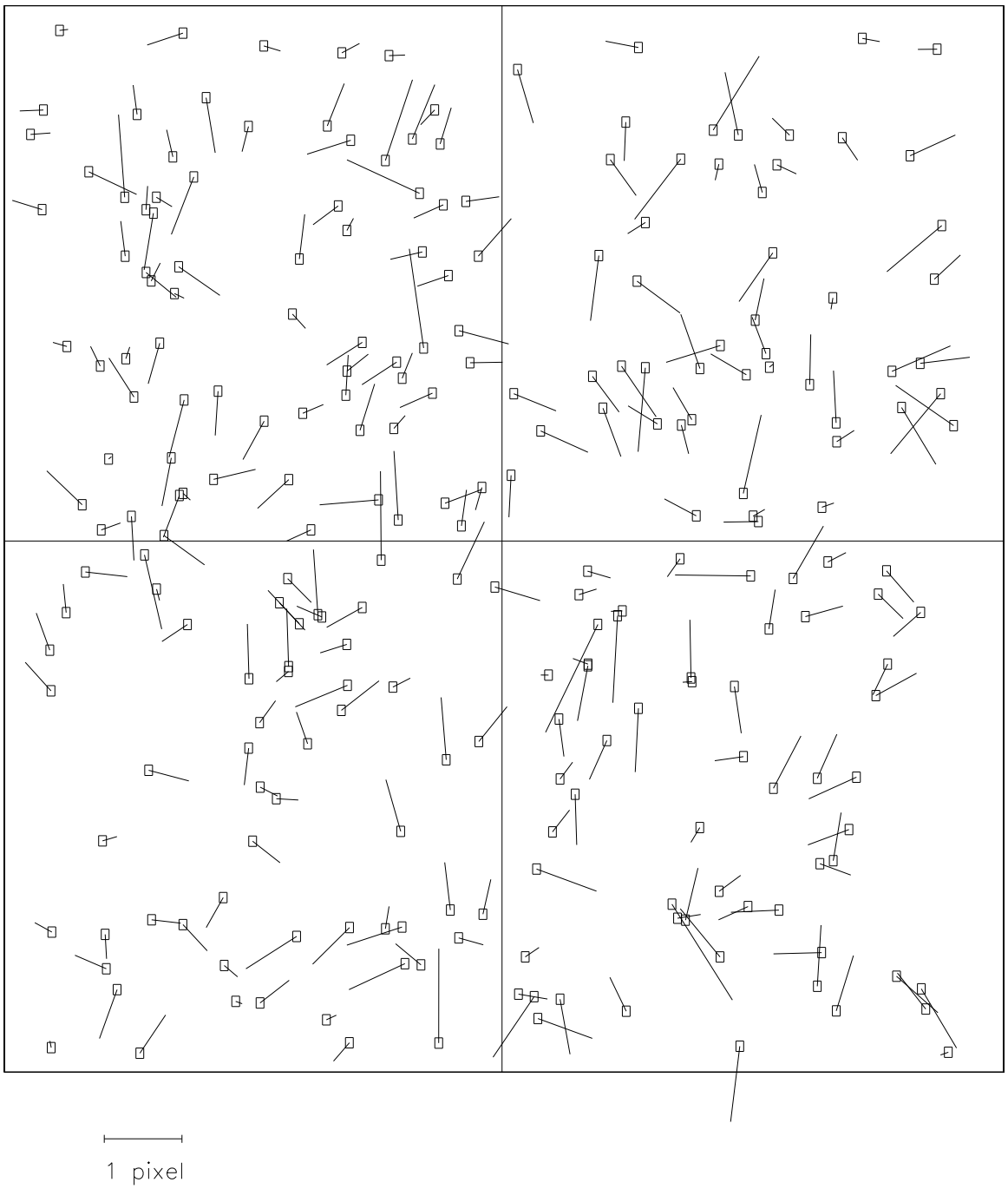

Figure 4. The residuals for the 256×256 model. The residuals are shown as magnified vectors showing the difference between the measured star position and the model-predicted star position. The boxes designate the tails of the vectors. The vectors are placed at the position in the raw image corresponding to the measured star position. The overplotted horizontal and vertical lines show the location of the *x* and *y* knots that segment the spline fitting region.

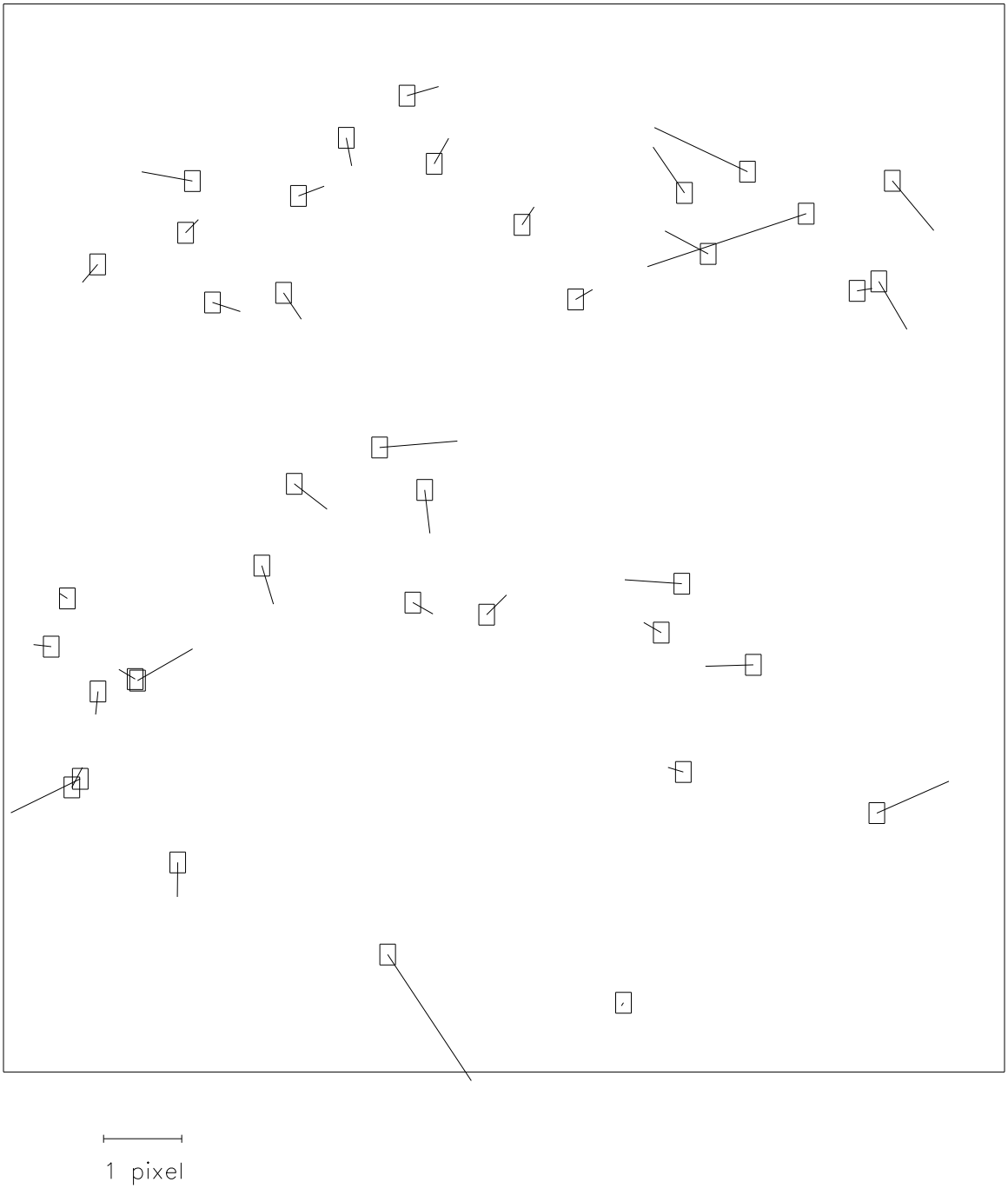

Figure 5. The residuals for the 128×128 model. The residuals are shown as magnified vectors showing the difference between the measured star position and the model-predicted star position. The boxes designate the tails of the vectors. The vectors are placed at the position in the raw image corresponding to the measured star position.

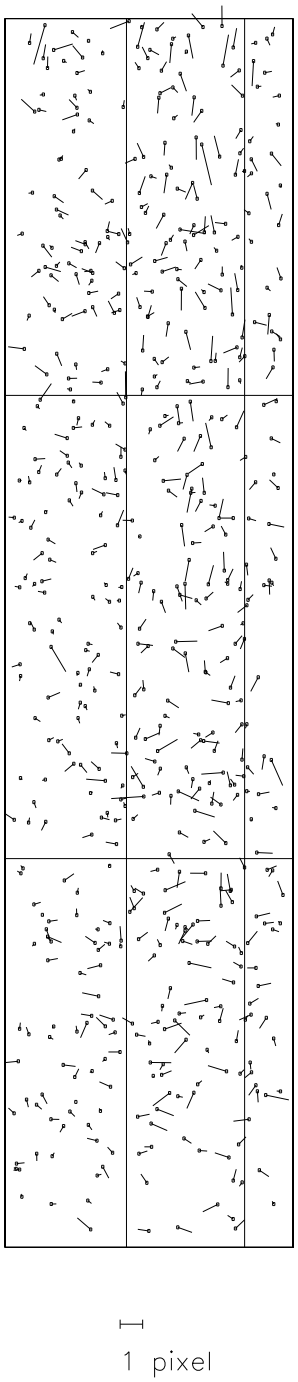

Figure 6. The residuals for the 256×1024 model. The residuals are shown as magnified vectors showing the difference between the measured star position and the model-predicted star position. The boxes designate the tails of the vectors. The vectors are placed at the position in the raw image corresponding to the measured star position. The overplotted horizontal and vertical lines show the location of the *x* and *y* knots that segment the spline fitting region.

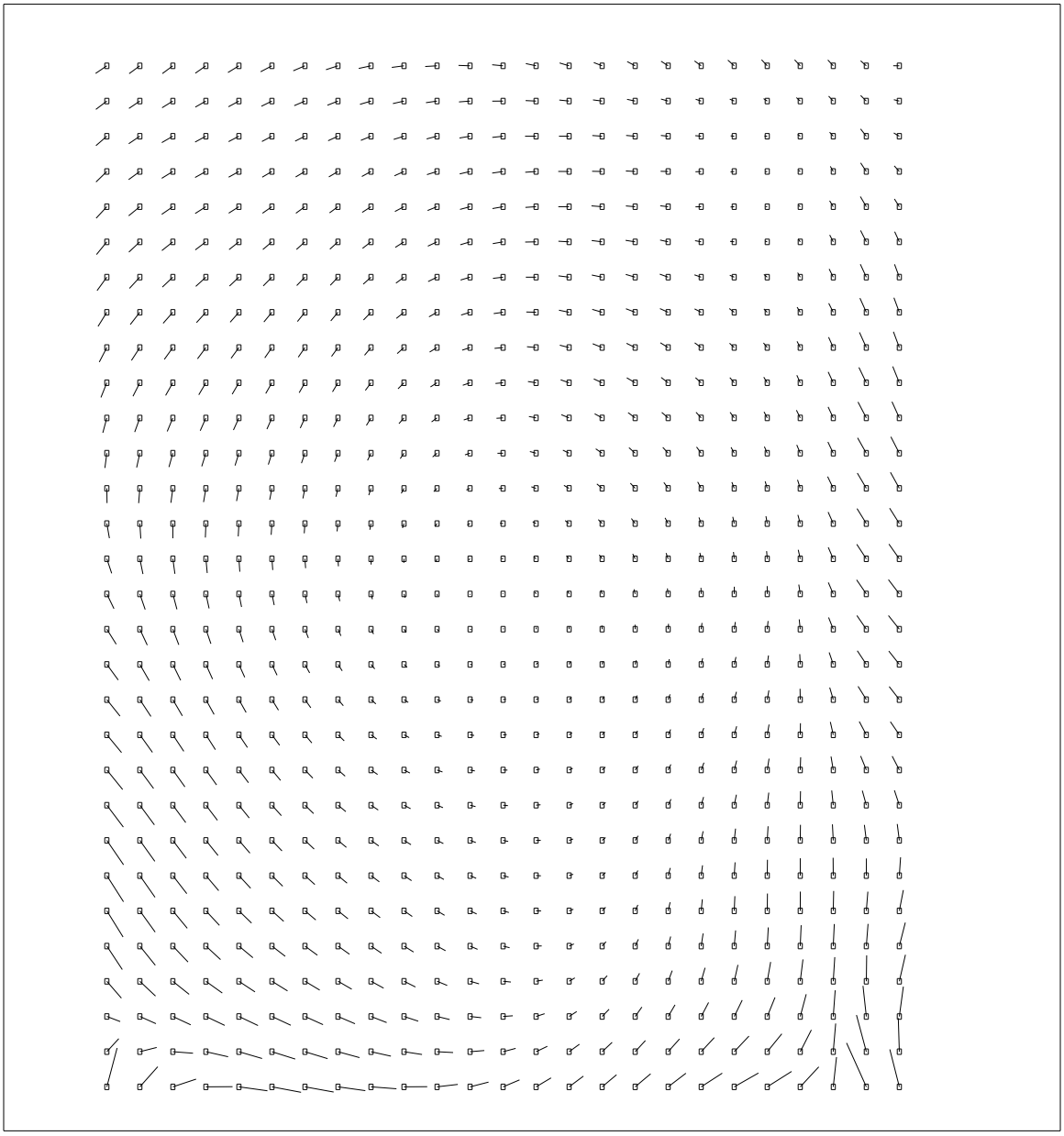

Figure 7. The difference between the new distortion model vectors and the distortion model vectors (ISR FOC-086) for the 512×512 format shown magnified on a grid with a spacing of 16 pixels. Because of the large distortion effects near the edges, the distortion differences are not shown near the edges.

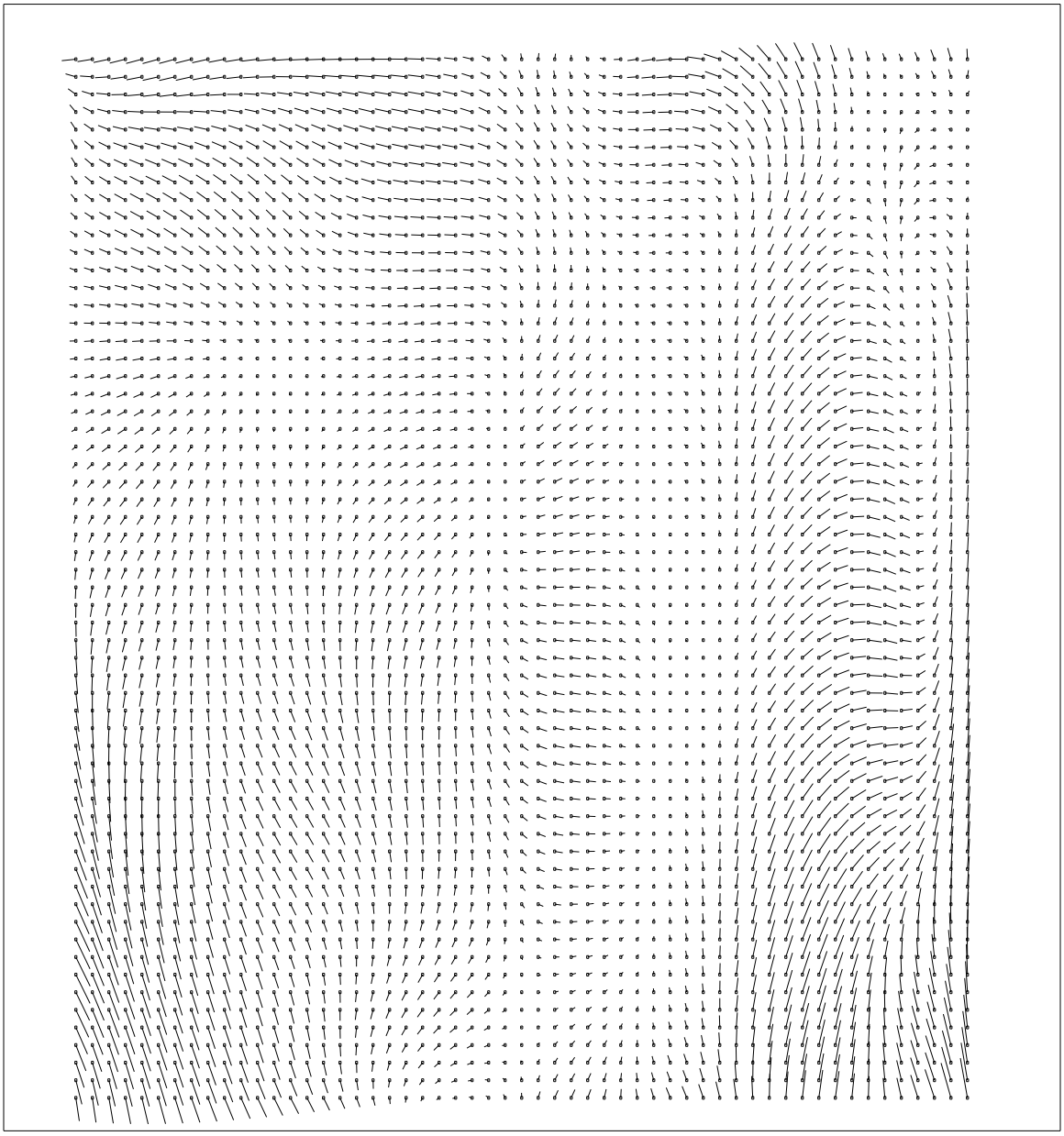

Figure 8. The difference between the new distortion model vectors and the distortion model vectors (ISR FOC-086) for the 512z×1024 format shown magnified on a grid with at spacing of 16 pixels (dezoomed). Because of the large distortion effects near the edges, the distortion differences are not shown near the edges.

ble. The amount of the drift in this case should not seriously affect the consistency of the solution since if we presume the drift was basically linear in plate scale versus time, the drift over any one of the series for a given format would be approximately a quarter of that observed between these two observations (which spanned over six hours). That would imply a net drift over a series of about 0.04% or about 0.5 pixels difference in the spacing of stars located at opposite edges of the format which is sufficiently small for the purposes of the fit.

6. Geometric Correction Files

The new distortion models were used to generate geometric correction files. Table 4 shows the new files and the files they replaced. The new files should be considered the ones to use for all post-COSTAR data. They were installed into the calibration pipeline on 19 March 1995. Because there is a different optical distortion resulting from the use of COSTAR, the flat fields used for pipeline calibration needed to be modified to match the current optical distortion correction. A "differential" geometric correction file was constructed to apply to the old flat field files to produce flat field files that match the current optical distortion correction. The new flat field correction files generated are listed in Table 5 with the files they replaced. The new flat field correction files were generated and installed into the calibration pipeline the same time the geometric correction files were.

7. Residual Photometric Effects

One of the motivations driving the new approach to determining the distortion model was the possibility of correcting for the fine scale variations in the flat field seen near the beginning of the scan line (the alternating bright and dark vertical bars seen near the right hand edge, see Figure 10 for example). The canonical explanation for these scan start-up variations was that they were the result of variations in the scan rate at the start of a scan. More specifically, variations in scan rate result in distortion, primarily in the *x*-direction. The varying size of pixels along the scan line direction results in varying apparent sensitivity as seen in flat fields. If this is indeed the case, a proper geometric correction would remove these flat field features.

The obvious question is: have these features been removed by the new geometric correction? Looking at a 512×512 LED flat field that has been geometrically corrected using the new model shows clearly that these features have not gone away as a result of the new geometric correction. This raises the question of whether the model is inadequate to model such variations or whether they do not arise from distortion. Figure 11 shows the average of all rows between y=200 and y=500 for both the raw image (upper curve) and the geometrically corrected image (lower curve). The corrected curve has been displaced by 0.4 to clearly separate it from the upper curve. Both have been normalized by the average value. The vertical lines mark the location of the x knots (which refer to their location relative to the raw image coordinates, i.e., the top curve). The beginning of scan variations show up clearly on the right edge of the plot starting with one large oscillation (~20% peak-to-peak) followed by three smaller ones (~10% peak-to-peak).

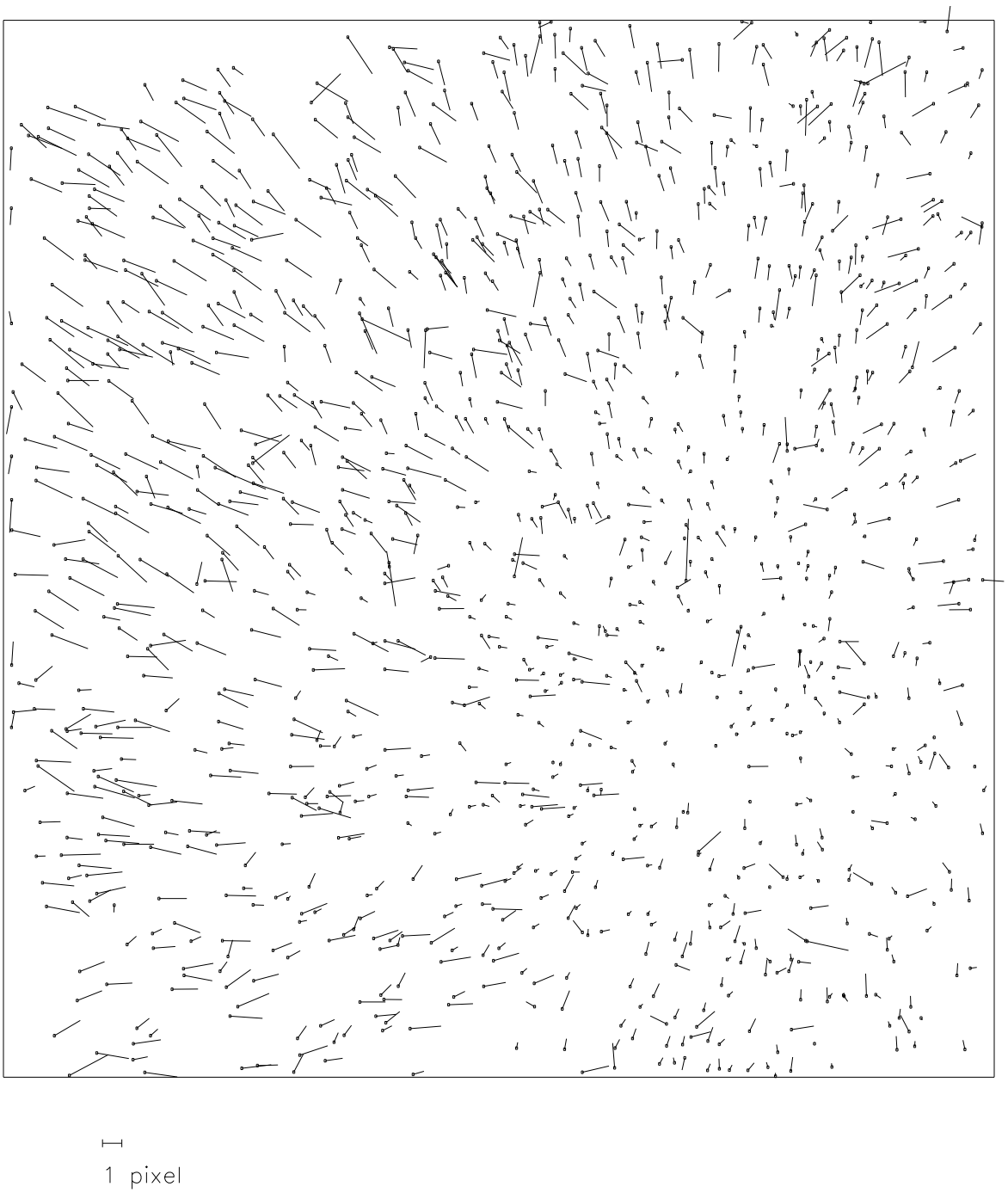

Figure 9. The difference in positions for stars shown as magnified vectors for two repeated exposures of the same field in 47 Tuc separated by more than 6 hours.

New Cal. Filename	Format	Cal. File Replaced
f3715310x.r5h	512z×1024	e8q0912mx.r5h
f371529ex.r5h	512×512	e8q09106x.r5h
f3715276x.r5h	256×256	e8q09090x.r5h
f371522px.r5h	128×128	N/A
f371522ex.r5h	256×1024	N/A

Table 4. The new geometric correction reference files and the files they replace. These files took effect 19 March 1995 in the calibration pipeline. They should be considered the files to use for all post-COSTAR FOC observations.

New Cal. Filename	Wavelength	Cal. File Replaced
f3716027x.r2h	1360 Å	c2410530x.r2h
f3716029x.r2h	4800	bbe14193x.r2h
f371602cx.r2h	5600	bbe14196x.r2h
f371602dx.r2h	6600	bbe14198x.r2h

Table 5. The new flat field correction reference files and the files they replace. These files took effect 19 March 1995 in the calibration pipeline. They should be considered the files to use for all post-COSTAR FOC observations.

Before concluding that these photometric features are not cause by distortion it is necessary to estimate whether they are measurable as distortion using the new method. Assuming that the distortion is sinusoidally periodic we can determine the peak distortion given the size of the photometric variation and its period in pixels. It is straightforward to show that the peak distortion D (deviation from a the average plate scale) for a one-dimensional sinusoidal distortion has the following relation to the period P and amplitude of photometric variation A (expressed as a fraction of the average level) $D=AP/2\pi$. For the smaller oscillations A is 0.05 and P is 16 resulting in a peak distortion of 0.12 pixels which would only be marginally noticeable in the residuals. The peak residuals for the first oscillation should be twice as large, i.e., 0.25 pixels, still relatively small but should be observable. Nevertheless it is not evident in the residuals.

This analysis by itself would not be terribly convincing by itself that the photometric oscillations are not a result of distortion. The major piece of evidence that argues against distortion as the explanation is a larger scale feature, the general 10% to 15% increase in brightness seen between pixels 410 and 470 on top of which the oscillations are present. This enhancement is clearly associated with the oscillations and is sizeable over many pixels. If it were due to distortion it should have been modeled, for unlike the small scale oscillations, it is of a size scale comparable to the knot spacing. A 10% average increase in brightness over 50 pixels would result in a 5-pixel dis-

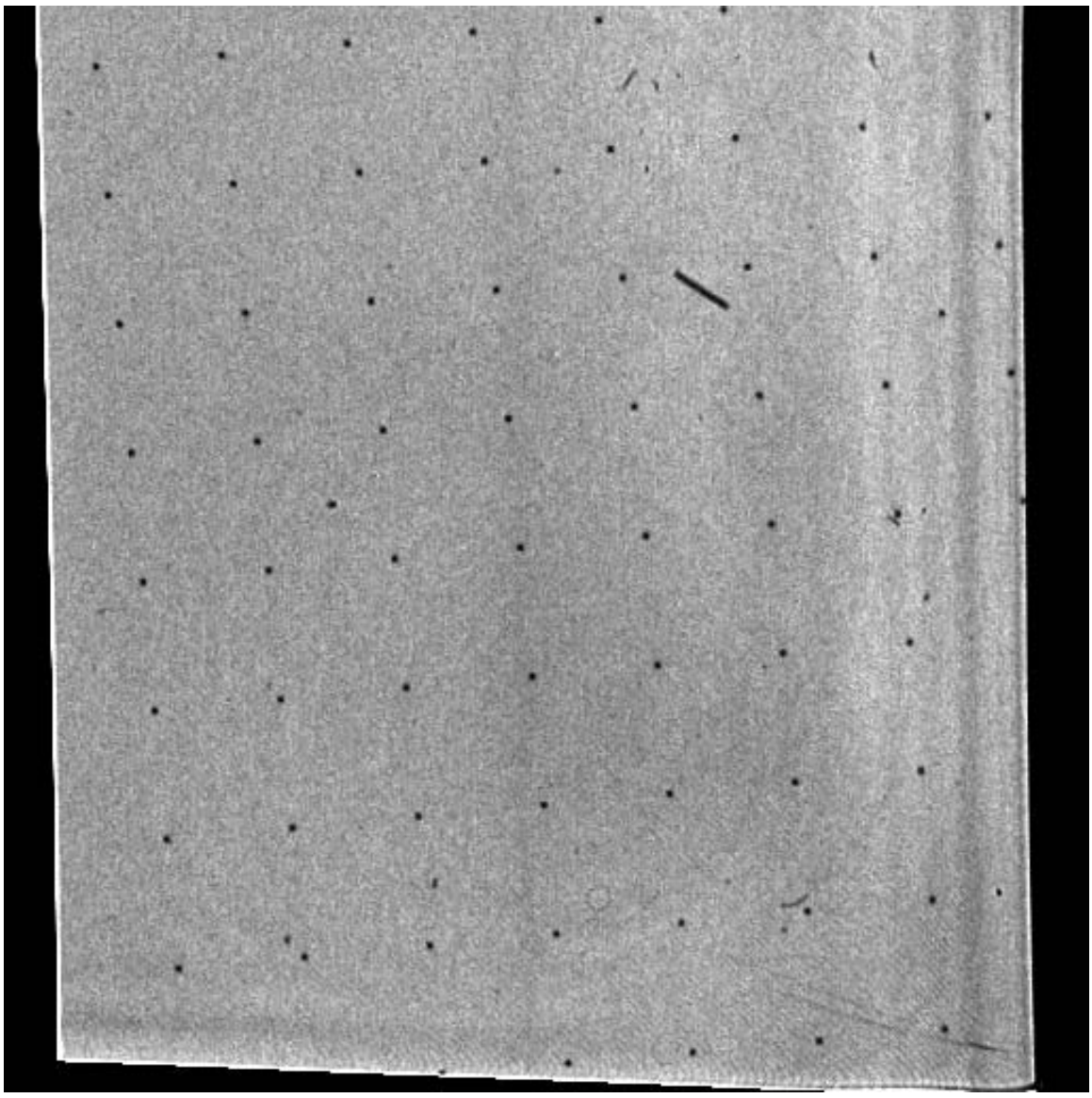

Figure 10. A 512×512 LED flat field that has been geometrically corrected using the latest geometric correction model. Note the photometric variations near the beginning of the scan line (the right hand edge) that appear as vertical features have not been removed as a result of the geometric correction.

tortion, a huge amount. Yet the corrected curve shows that there is relatively little change in the relative brightness. This shows that the model did not remove the effect, and the residuals show no evidence that the model missed the presumed geometric effect. This is powerful evidence that the photometric effects at the beginning of the scan line are not due entirely to distortion effects; in fact, it is apparent that very little of it, if any, is due to distortion effects. Whatever the cause, it must be indirectly related to the scan line sweep rate, that is, a small variation in scan rate has some large indirect effect on sensitivity.

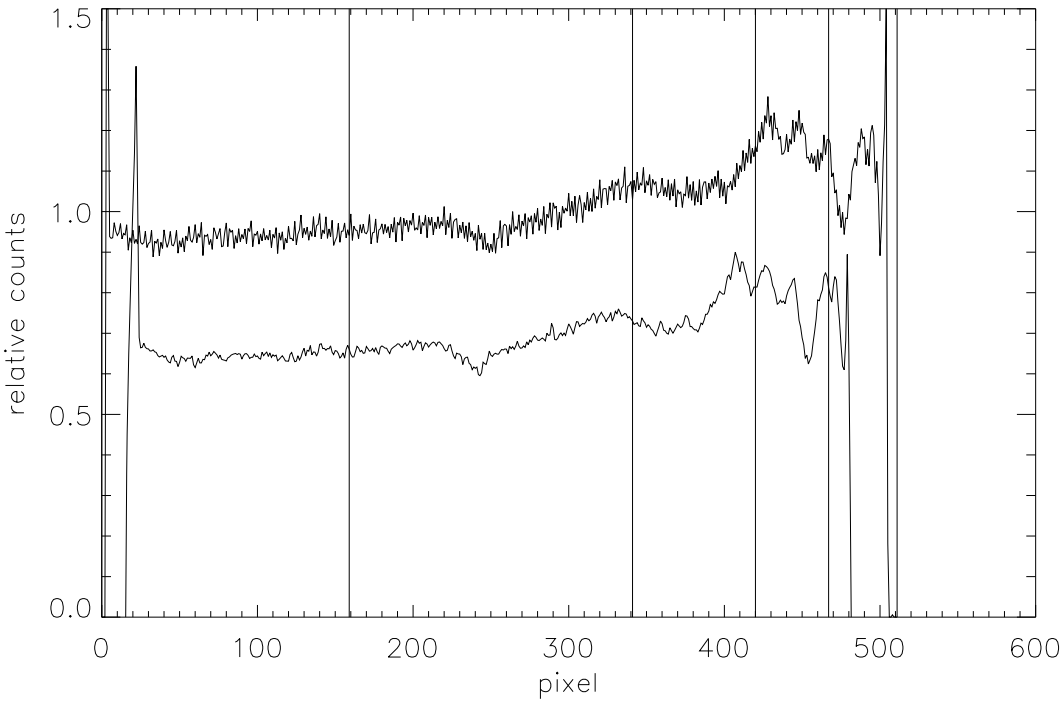

Figure 11. The average of rows 200 through 500 of the 512×512 LED flat field. The top curve shows the average for the raw image while the lower curve shows the average for the geometrically corrected image. Both curves have been normalized by the average value in the averaged region. The lower curve has been offset by 0.4 to clearly separate it from the upper curve. The vertical lines show the location of the *x* knots which are valid only for raw image coordinates.

8. References

1. Greenfield, P., Instrument Science Report FOC-086, *Deriving the Geometric Correction from Crowded Fields*, 15 February 1995.

2. Greenfield, P., Instrument Science Report FOC-088, *A Description of the Software used to Derive the Geometric Correction*, 12 September 1995.

9. Appendix

Tables 4-8 list the distortion model coefficients for the different formats. Refer to Instrument Science Report FOC-088 for an explanation of how to use the spline coefficients to apply the distortion correction. Since the spline fits generate a distortion correction which has an arbitrary offset, applying an offset is necessary to register the correction with other formats (and by implication, set the overall registration, which I have taken to match the previous full format distortion correction). The coefficients for the 128×128 format are used in a 2-dimensional polynomial which is defined as

$$f = c_0 + c_1x + c_2y + c_3x^2 + c_4xy + c_5y^2.$$

		0	1	2	3	4	5	6	7	8	9	10
x:	0	-335.3777	-294.4028	-220.0122	-137.7627	-74.6514	-21.9114	35.8766	83.3888	121.8391	140.8901	158.4359
	1	-335.5470	-294.6411	-221.1190	-139.2623	-76.5960	-24.7699	32.5531	81.3252	117.7703	141.4733	150.3053
	2	-336.6700	-295.9409	-223.9097	-143.4431	-80.8980	-28.6400	28.7800	75.9615	114.4685	134.4923	148.5208
	3	-340.4296	-300.1554	-226.9872	-145.2825	-82.7836	-30.6043	26.3263	75.2299	112.3768	135.3084	145.8864
	4	-348.1082	-307.0546	-232.7321	-150.1066	-86.0276	-32.5104	27.2513	75.8467	115.6780	136.6391	151.0307
	5	-349.6896	-308.8469	-236.4470	-152.0013	-87.2978	-32.9190	27.1183	78.7278	118.5663	143.1199	154.0493
y:	0	-606.8826	-607.1485	-609.8506	-614.5410	-620.2610	-624.4877	-633.3167	-632.3627	-642.3163	-638.1720	-638.9640
	1	-501.7147	-501.5342	-505.1399	-510.4167	-516.2632	-519.3739	-526.0953	-527.4296	-531.3765	-530.2935	-528.0785
	2	-258.8111	-260.4648	-264.8695	-270.1564	-275.8738	-278.5222	-284.4624	-281.5574	-286.2589	-282.4141	-276.9131
	3	98.6047	94.3756	86.4956	81.2116	76.5211	76.2930	72.5325	77.8506	74.8378	81.6228	83.3578
	4	363.4758	359.7860	347.1910	341.6883	336.1764	337.0558	335.0323	341.5379	341.2943	345.0512	353.8827
	5	495.7200	482.1450	468.7441	460.6934	455.0268	455.1176	451.8534	457.8040	454.6922	462.1972	462.0476

Table 6. The distortion model coefficients for the 512*z*×1024 format. These spline coefficients are used to translate the raw, distorted, zoomed coordinates into undistorted zoomed coordinates. To generate the translation between dezoomed coordinates it necessary to divide the *x* coordinate by 2, use the above defined transformation and then multiply the resulting *x* coordinate by 2. Finally an offset of 713.75, 605.05 must be added to the *x,y* coordinates.

		0	1	2	3	4	5	6	7
x:	0	-277.8163	-230.6939	-127.9230	-1.9516	94.0992	149.5876	178.9515	192.4354
	1	-278.6607	-230.6110	-128.6591	-3.4270	93.6152	147.0999	177.2429	191.2976
	2	-279.6118	-234.7947	-130.7464	-5.2146	90.4180	146.4820	174.9105	189.2814
	3	-284.6721	-235.8037	-134.2955	-7.6732	89.6568	143.2984	172.0329	189.5963
	4	-287.4205	-240.9640	-136.5205	-9.7565	86.9572	143.2423	173.0443	184.5473
	5	-289.2265	-242.5367	-137.6575	-10.9817	87.2798	142.6642	170.0594	191.7626
y:	0	-117.8632	-118.9170	-123.9690	-128.1461	-132.2248	-131.4605	-137.3464	-129.4594
	1	-68.9852	-71.1555	-74.8196	-80.5303	-84.1685	-83.6478	-87.4229	-77.9673
	2	53.4630	52.5330	46.9123	43.7284	40.4486	39.9230	38.5806	40.8678
	3	227.1560	224.2442	221.3669	215.1190	213.5247	214.6154	210.4180	221.3669
	4	353.6387	352.2208	345.6836	343.4112	341.0799	341.9911	340.1939	344.2387
	5	404.0305	401.3763	397.2847	392.1207	390.7592	393.4785	388.2157	398.7874

Table 7. The distortion model coefficients for the 512×512 format. After applying the transformation defined by these coordinates is necessary to add the offset 300.85, 131.72 to the resulting coordinates.

		0	1	2	3	4
x:	0	-163.513	-124.600	-46.8961	28.6725	70.0034
	1	-165.032	-124.428	-50.5662	31.8930	64.2634
	2	-165.271	-127.407	-47.1502	26.5015	70.6125
	3	-169.135	-126.024	-53.5315	29.0873	64.5162
	4	-166.434	-130.732	-48.4659	24.2038	66.8202
y:	0	4.00661	3.90794	-0.204523	-0.798520	-1.32415
	1	48.1036	46.7047	44.8028	40.4506	42.5996
	2	133.506	129.464	129.261	126.892	129.382
	3	216.608	218.638	214.633	209.708	213.094
	4	263.556	259.084	259.110	256.014	258.178

Table 8. The distortion model coefficients for the 256×256 format. After applying the transformation defined by these coordinates is necessary to add the offset 172.85, 3.72to the resulting coordinates.

		0	1	2	3	4	5
x:	0	-311.384	-277.802	-214.822	-134.213	-91.1200	-74.5506
	1	-315.303	-281.894	-217.848	-140.138	-96.2336	-82.4975
	2	-322.152	-288.489	-225.454	-147.441	-103.860	-88.5535
	3	-326.260	-292.254	-229.833	-150.227	-107.051	-94.6133
	4	-336.418	-301.237	-236.485	-156.716	-111.490	-93.7263
	5	-340.370	-303.482	-240.657	-157.099	-113.944	-96.6036
y:	0	-601.382	-602.797	-605.890	-609.125	-609.415	-607.435
	1	-492.857	-494.001	-495.813	-499.217	-499.635	-498.949
	2	-253.216	-255.653	-257.316	-260.771	-260.525	-260.020
	3	89.7133	88.7008	86.9394	84.6335	84.7821	88.9437
	4	336.853	336.913	332.982	332.785	331.670	334.570
	5	454.543	450.273	449.126	445.020	446.465	447.250

Table 9. The distortion coefficients for the 256×1024 format.After applying the transformation defined by these coordinates is necessary to add the offset 329.10, 605.05 to the resulting coordinates.

	x	***y***
c_0	2.935	4.9309
c_1	0.861428	-4.276848e-2
c_2	-1.210785e-2	0.996674
c_3	3.650710e-4	1.652092e-4
c_4	-1.437217e-5	-3.533065e-5
c_5	3.802776e-5	-1.406670e-5

Table 10. The distortion coefficients for the 128×128 format.